Inorg. Chem. **2008**, *47*, 10269−10279

Design of Dipicolinic Acid Ligands for the Two-Photon Sensitized Luminescence of Europium Complexes with Optimized Cross-Sections

Anthony D'Aléo,[†] Alexandre Picot,[†] Patrice L. Baldeck,[‡] Chantal Andraud,[†,*] and Olivier Maury[†,*]

Université de Lyon, Laboratoire de Chimie, CNRS - Ecole Normale Supérieure de Lyon, UMR 5182, 46 allée d'Italie, 69007 Lyon, France, and Laboratoire de Spectrométrie Physique, Université Joseph Fourier, CNRS - UMR 5588, BP 87 F-38402 Saint Martin d'Hères, France

Received July 10, 2008

The multistep synthesis of an extensive series of push−pull donor-π-conjugated dipicolinic acid ligands is described. The charge transfer character of the ligand can be tuned by changing the donor group (CH_2R, OR, SR, or NR_2) or the nature of the conjugated backbone (phenyl, phenylethynyl, naphtylethynyl, bis(phenylethynyl), or chalcone). The photophysical properties of related D_3 symmetric europium complexes (absorption and luminescence) were measured. Experiments using two-photon sensitized luminescence of a Eu^{III} complex reveal large two-photon absorption (TPA) cross-section values (775 GM at 740 nm) in dichloromethane. Furthermore, some structure−property relationships can be derived from this systematic study, allowing an optimization of TPA properties of lanthanide complexes.

Introduction

Since the pioneering work of Webb in the early 1990s,[1] two-photon excited microscopy has evolved as an alternative to conventional techniques for in vivo, in vitro, or in cellulo biological imaging[2−5] or sensing[6−10] (pH,[11] Mg^{2+},[12,13] Zn^{2+},[14]...) applications. This technique is based on the two-photon excited fluorescence phenomenon that consists of the simultaneous absorption of two photons of longer wavelength (TPA; a third-order nonlinear optical phenomenon) followed by the classical emission of a fluorescence photon. The spatial confinement of two-photon laser excitation presents several intrinsic advantages: three-dimensional resolution and reduced photobleaching and photodamage due to the absence of out-of-focus absorption. In addition, longer-wavelength near-infrared (NIR) light (typically 800 nm) used for TPA excitation is less scattered by biological tissue, allowing deeper penetration.[15] This technique requires the presence of fluorescent probes that can be either an endogenous dye or commercially available fluoro-probes featuring a generally low two-photon absorption cross-section (σ_2 < 50 GM).[16] For a decade, chromophores have been specially optimized for such applications with a high σ_2 value comprised between 750 and 1500 GM for organic dyes[17−23] and up to 50 000 GM for quantum dots or dendrimers.[24,25]

On the other hand, lanthanide complexes have been widely and successfully used for bioimaging,[26−30] taking benefit

* Author to whom correspondence should be addressed. E-mail: olivier.maury@ens-lyon.fr.
† Université de Lyon.
‡ Université Joseph Fourier.

(1) Denk, W.; Strickler, J. H.; Webb, W. W. *Science* **1990**, *248*, 73–76.
(2) Vaganova, E.; Yitzchaik, S.; Sigalov, M.; Borst, J. W.; Visser, A.; Ovadia, H.; Khodorkovsky, V. *New J. Chem.* **2005**, *29*, 1044–1048.
(3) Krishna, T. R.; Parent, M.; Werts, M. H. V.; Moreaux, L.; Gmouh, S.; Charpack, S.; Caminade, A.-M.; Majoral, J.-P.; Blanchard-Desce, M. *Angew. Chem., Int. Ed.* **2006**, *45*, 4645–4648.
(4) Hayek, A.; Ercelen, S.; Zhang, X.; Bolze, F.; Nicoud, J.-F.; Schaub, E.; Baldeck, P. L.; Mély, Y. *Bioconjugate Chem.* **2007**, *18*, 844–851.
(5) Mathai, S.; Bird, D. K.; Stylli, S. S.; Smith, T. A.; Ghiggino, K. *Photchem. Photobiol. Sci.* **2007**, *6*, 1019–1026.
(6) Campagnola, P. J.; Loew, L. M. *Nat. Biotechnol.* **2003**, *21*, 1356–1360.
(7) Zipfel, W. R.; Williams, R. M.; Webb, W. W. *Nat. Biotechnol.* **2003**, *21*, 1356–1360.
(8) Mertz, J. *Curr. Opin. Neurobiol.* **2004**, *14*, 610–616.
(9) Rubart, M. *Circ. Res.* **2004**, *95*, 1154–1166.
(10) Yuste, R. *Nat. Methods* **2005**, *2*, 902–904.
(11) Werts, M. H. V.; Gmouh, S.; Mongin, O.; Pons, T.; Blanchard-Desce, M. *J. Am. Chem. Soc.* **2004**, *126*, 16294–16295.
(12) Farruggia, G.; Iotti, S.; Prodi, L.; Montalti, M.; Zaccheroni, N.; Savage, P. B.; Trapani, V.; Sale, P.; Wolf, F. I. *J. Am. Chem. Soc.* **2006**, *128*, 344–350.
(13) Kim, H. M.; Yang, P. R.; Seo, M. S.; Yi, J.-S.; Hong, J. H.; Jeon, S.-J.; Ko, Y.-G.; Lee, K. J.; Cho, B. R. *J. Org. Chem.* **2007**, *72*, 2088–2096.
(14) Chang, C. J.; Nolan, E. M.; Jaworski, J.; Okamoto, K.-I.; Hayashi, Y.; Sheng, M.; Lippart, S. *J. Inorg. Chem.* **2004**, *43*, 6774–6779.
(15) Levene, M. J.; Dombeck, D. A.; Kasische, K. A.; Molloy, R. P.; Webb, W. W. *J. Neurophysiol.* **2004**, *91*, 1908–1912.
(16) Xu, C.; Zipfel, W.; Shear, J. B.; Williams, R. M.; Webb, W. W. *Proc. Natl. Acad. Sci.* **1996**, *93*, 10763–10768.

10.1021/ic8012975 CCC: $40.75
Published on Web 10/21/2008

from the very characteristic luminescence properties of these metal ions[31−35] (sharp transitions with a large Stokes shift located in the visible or in the NIR spectral range, insensitivity to oxygen, and sensitivity to the local environment) and particularly from their long excited-state lifetime. This latter property triggered the development of time-gated microscopy in order to eliminate any parasitic short-lived luminescence coming from the scattering or autofluorescence of endogenous chromophores or other molecular probes.[30,36−40] In order to combine the advantages of both rare earths and nonlinear microscopy, our project was to design a new generation of lanthanide complexes stable in biological media and featuring optimized two-photon cross-sections. In the early 2000s, the groups of Lakowicz and Thompson, respectively, demonstrated the proof-of-concept of a two-photon antenna effect in a biological medium with complexes exhibiting very low (generally not measured) TPA cross-sections.[41,42] Recently, sensitization of europium(III) was achieved by the two-photon antenna effect, using either Michler's ketone,[43] 2-(diethylanilin-4-yl)-4,6-bis(3,5-dimethylpyrazolyl)-triazine,[44,45] or functionalized pyridine-dicarboxamide ($\mathbf{L^{2A}}$, Chart 1). [46] In all cases, σ_2 values are significant, comprised between 100 and 300 GM, but these complexes are only stable in organic solvents and not compatible with water and therefore are not suitable for any practical applications as biological probes. To overcome this limitation, we focused on tris-dipicolinate lanthanide complexes $Ln(DPA)_3^{3-}$ (DPA = 2,6-pyridine-dicarboxylic acid, Chart 1) known to present sufficient stability in water for spectroscopic applications,[47,48] and we described the first two-photon microscopy experiment of a $Tb(DPA)_3^{3-}$ derived-protein crystal.[49] On the other hand, Wong et al. described the sensitization of terbium by the three-photon antenna effect to image biological cells.[50] In addition, Palsson et al. reported two-photon excited time-resolved luminescence spectroscopy experiments using a cavity dumped Ti-sapphire laser source.[51] This important result opens the way for the development of time-gated two-photon microscopy imaging techniques. It is important to note that all of these complexes used for nonlinear microscopy bioimaging present a rather low two- (respectively three-) photon cross-section (for instance, with a TPA cross-section < 5 GM), which is a main drawback for practical applications. In this context, functionalization of the DPA ligand by (i) a π-conjugated TPA antenna and (ii) hydrosolubilizing groups ($\mathbf{L^{2G}}$, Chart 1) has allowed the synthesis of the europium complex $Na_3[Eu(\mathbf{L^{2G}})_3]$ featuring significant σ_2 in water (92 GM at 700 nm) and suitable for two-photon microscopy imaging of fixed human cancer cells.[52] To further optimize the properties of this class of complexes, it is important to increase the TPA cross-section of the probe at the bioimaging operating wavelengths that are comprised between 700 and 1000 nm for Ti-Sapphire fs-laser and more precisely in the 750−800 spectral range usually used for practical imaging experiments.

In this study, the spectroscopic properties of a series of dipolar ligands, D-π-A ($\mathbf{L^1}$−$\mathbf{L^9}$), and the corresponding $[NBu_4]_3[Eu(\mathbf{L}^i)_3]$ (i = 1−9) complexes were studied, in which the acceptor part (A) is the dipicolinic acid fragment and in which the strength of the donor (D = dialkylamino,

(17) Mongin, O.; Porres, L.; Charlot, M.; Katan, C.; Blanchard-Desce, M. *Chem.—Eur. J.* **2007**, *13*, 1481–1498.
(18) Hayek, A.; Nicoud, J.-F.; Bolze, F.; Bourgogne, C.; Baldeck, P. L. *Angew. Chem., Int. Ed.* **2006**, *45*, 6466–6469.
(19) Barsu, C.; Fortrie, R.; Nowika, K.; Baldeck, P. L.; Vial, J.-C.; Barsella, A.; Fort, A.; Hissler, M.; Bretonnière, Y.; Maury, O.; Andraud, C. *Chem. Commun.* **2006**, 4744–4746.
(20) Kim, H. M.; Yang, W. J.; Kim, C. H.; Park, W.-H.; Jeon, S.-J.; Cho, B. R. *Chem.—Eur. J.* **2005**, *11*, 6386–6391.
(21) Chung, S.-J.; Rumi, M.; Alain, V.; Barlow, S.; Perry, J. W.; Marder, S. R. *J. Am. Chem. Soc.* **2005**, *127*, 10844–10845.
(22) Nielsen, C. B.; Johnsen, M.; Arnbjerg, J.; Pittelkow, M.; McIlroy, S. P.; Ogilby, P. R.; Jorgensen, M. *J. Org. Chem.* **2005**, *70*, 7065–7079.
(23) Bartholomew, G. P.; Rumi, M.; Pond, S. J. K.; Perry, J. W.; Tretiack, S.; Bazan, G. C. *J. Am. Chem. Soc.* **2004**, *126*, 11529–11542.
(24) Mongin, O.; Krishna, T. R.; Werts, M. H. V.; Caminade, A.-M.; Majoral, J.-P.; Blanchard-Desce, M. *Chem. Commun.* **2006**, 915–917.
(25) Larson, D. R.; Zipfel, W. R.; Williams, R. M. W. C. S.; Bruchez, M. P.; Wise, F. W.; Webb, W. W. *Science* **2003**, *300*, 1434–1436.
(26) Yu, J.; Parker, D.; Pal, R.; Poole, R. A.; Cann, M. J. *J. Am. Chem. Soc.* **2006**, *128*, 2294–2299.
(27) Charbonnière, L. J.; Hildebrandt, N.; Ziessel, R.; Löhmannsröben, H. G. *J. Am. Chem. Soc.* **2006**, *128*, 12800–12809.
(28) Aarons, R. J.; Notta, J. K.; Meloni, M. M.; Feng, J.; Vidyasagar, R.; Narvainen, J.; Allan, S.; Spencer, N.; Kauppinen, R. A.; Snaith, J. S.; Faulkner, S. *Chem. Commun.* **2006**, 909–911.
(29) Weibel, N.; Charbonnière, L. J.; Guardigli, M. A. R.; Ziessel, R. *J. Am. Chem. Soc.* **2004**, *126*, 4888–4896.
(30) Charbonnière, L. J.; Weibel, N.; Estournes, C.; Leuvrey, C.; Ziessel, R. *New. J. Chem.* **2004**, *28*, 777–781.
(31) Bünzli, J.-C. G. *Acc. Chem. Res.* **2006**, *39*, 53–61.
(32) Pandya, S.; Yu, J.; Parker, D. *Dalton Trans.* **2006**, 2757–2766.
(33) Gunnlaugsson, T. L. J. P. *Chem. Comm.* **2005**, *25*, 3114–3131.
(34) Faulkner, S.; Pope, S. J. A.; Burton-Pye, B. P. *Appl. Spec. Rev.* **2004**, *40*, 1–31.
(35) Parker, D. *Chem. Soc. Rev.* **2004**, *33*, 156–165.
(36) Marriot, G.; Clegg, R. M.; Arnt-Jovin, D. J.; Jovin, T. *Biophys. J.* **1991**, *60*, 1374–1387.
(37) Yuan, J.; Wang, G. *J. Fluoresc.* **2005**, *4*, 559–568.
(38) Vereb, G.; Jares-Reijman, E.; Selvin, P. R.; Jovin, T. M. *Biophys. J.* **1998**, *74*, 2210–2222.
(39) Phimphivong, S.; Saavedra, S. S. *Bioconjugate Chem.* **1998**, *9*, 350–357.
(40) Beeby, A.; Botchway, S. W.; Clarkson, I. M.; Faulkner, S.; Parker, A. W.; Parker, D.; Williams, J. A. G. *J. Photochem. Photobiol. B* **2000**, *57*, 83–89.
(41) White, G. F.; Litvinenko, K. L.; Meech, S. R.; Andrews, D. L.; Thomson, A. J. *Photochem. Photobiol. Sci.* **2004**, *3*, 47–55.
(42) Piszczek, G.; Maliwal, B. P.; Gryczynski, I.; Dattelbaum, J.; Lakowicz, J. R. *J. Fluoresc.* **2001**, *11*, 101–107.
(43) Werts, M. H. V.; Nerambourg, N.; Pélégry, D.; Le Grand, Y.; Blanchard-Desce, M. *Photochem. Photobiol. Sci.* **2005**, *4*, 531–538.
(44) Fu, L.-M.; Wen, X.-F.; Ai, X.-C.; Sun, Y.; Wu, Y.-S.; Zhang, J.-P.; Wang, Y. *Angew. Chem., Int. Ed.* **2005**, *44*, 747–750.
(45) Hao, R.; Li, M.; Wang, Y.; Zhang, J.; Ma, Y.; Fu, L.; Wen, X.; Wu, Y.; Ai, X.; Zhang, S.; Wei, Y. *Adv. Funct. Mater.* **2007**, *17*, 3663–3669.
(46) Picot, A.; Malvolti, F.; Le Guennic, B.; Baldeck, P. L.; Williams, J. A. G.; Andraud, C.; Maury, O. *Inorg. Chem.* **2007**, *46*, 2659–2665.
(47) Chauvin, A.-S.; Gumy, F.; Imbert, D.; Bünzli, J.-C. G. *Spetrosc. Lett.* **2004**, *37*, 517–532.
(48) Lessmann, J. J.; Horrocks, J. W. D. *Inorg. Chem.* **2000**, *39*, 3114–3124.
(49) D'Aléo, A.; Pompidor, G.; Elena, B.; Vicat, J.; Baldeck, P. L.; Toupet, L.; Kahn, R.; Andraud, C.; Maury, O. *ChemPhysChem* **2007**, *8*, 2125–2132.
(50) Law, G.-L.; Wong, K.-L.; Man, C. W.-Y.; Wong, W.-T.; Tsao, S.-W.; Lam, M. H.-W.; Lam, P. K.-S. *J. Am. Chem. Soc.* **2008**, *130*, 3714–3715.
(51) Palsson, L. O.; Pal, R.; Murray, B. S.; Parker, D.; Beeby, A. *Dalton Trans.* **2007**, 5726–5730.
(52) Picot, A.; D'Aléo, A.; Baldeck, P. L.; Grichine, A.; Duperray, A.; Andraud, C.; Maury, O. *J. Am. Chem. Soc.* **2008**, *130*, 1532–1533.

Chart 1. Chemical Structure and Abbreviation Name of the Studied Ligand and Related Eu^{III} Complexes

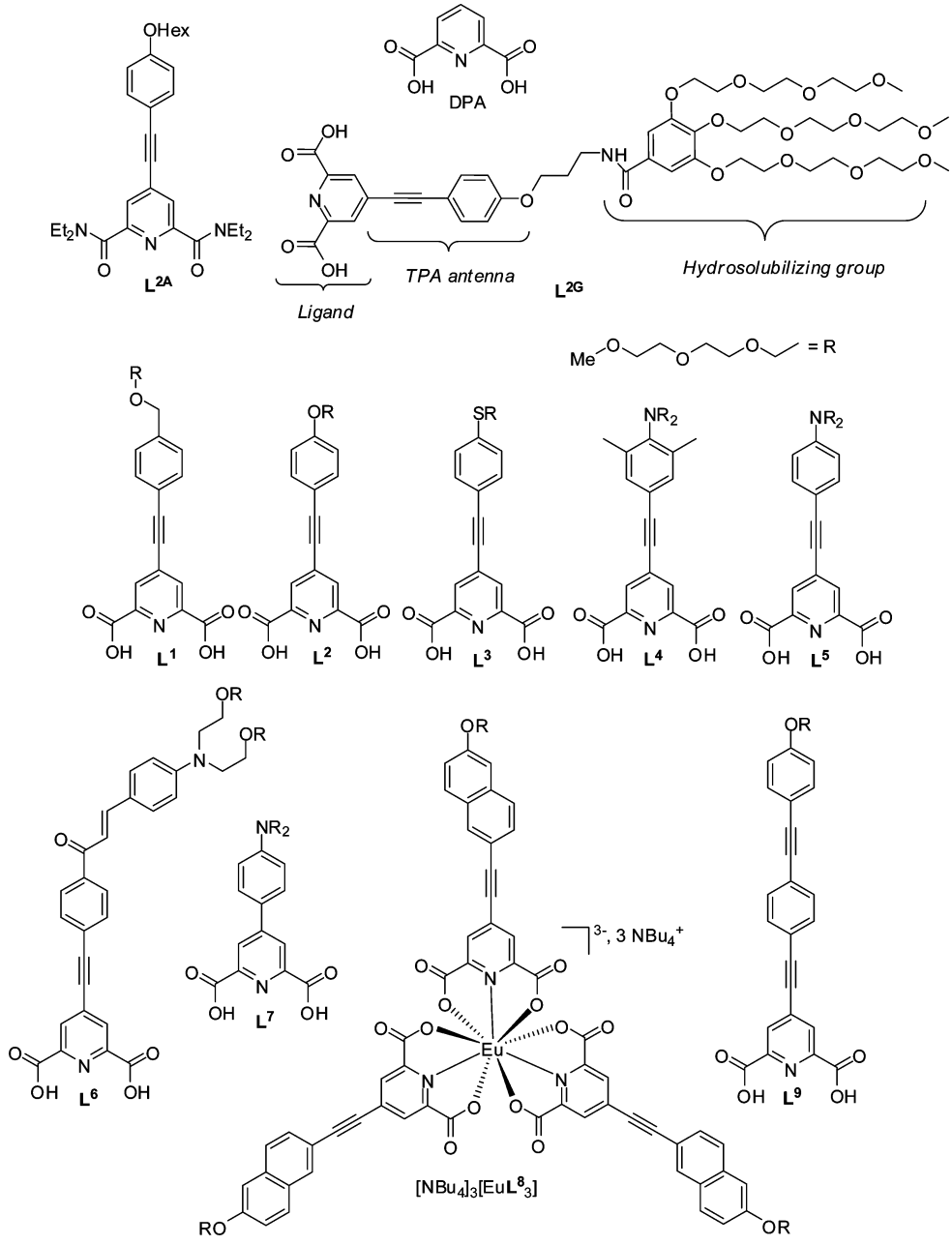

alkoxy, and alkylthio) as well as the length of the π-conjugated backbone (phenyl, phenylethynyl, naphtylethynyl, bis(phenylethynyl), and chalcone) could be tuned (Chart 1). Part 1 of this series of papers illustrated that the europium luminescence can be efficiently sensitized from a relaxed charge transfer (CT) excited state and that high quantum yields can been obtained (up to 40%) only when the CT excited-state energy lies above a limit estimated between 18 400 and 17 500 cm^{-1}. For this reason, this process can not occur in the case of the $[NBu_4]_3[Eu(\mathbf{L^6})_3]$ for which CT relaxed state energy is below this range. The second part of this work described in the present paper, consists in the systematic study of TPA properties of this family of europium complexes $[NBu_4]_3[Eu(\mathbf{L^{1-9}})_3]$ (Chart 1) in order (i) to red-shift the maximal TPA wavelength (λ_{TPA}) and (ii) to enhance the TPA cross-section.

Results

1. Synthesis. All of the ligands, $\mathbf{L^1}-\mathbf{L^9}$, are dipolar compounds in which an acceptor moiety, namely, dipicolic acid, is linked to various donor fragments, alkoxy, alkylthio, and dialkylamino, via a different π-conjugated skeleton. The synthesis involves as key steps palladium-catalyzed aryl/ethynyl Sonogashira or aryl/aryl Suzuki cross-coupling reactions. All of the syntheses started with the alkylation of commercially available compounds (4-iodophenol, 4-iodothiophenol, 6-bromo-2-naphtol, 2,6-dimethyl-4-bromoaniline, and 4-iodoaniline) with a [2-(2-(2-methoxyethoxy)ethoxy)-ethyl] group. This polyether chain was chosen to ensure the solubility of the ligand in water in order to carry out efficiently the final complexation step. Alkylation was performed in a basic medium using 2-(2-(2-methoxyethoxy)-

Scheme 1. Synthesis of the Conjugated Donor Groups **1**−**5c** and **8c**

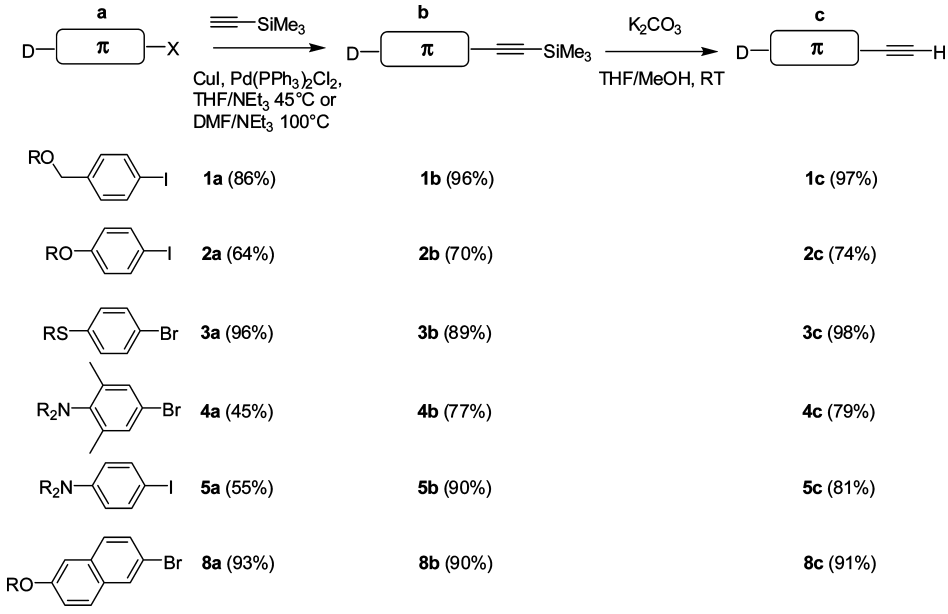

Scheme 2. Elongation of the π-Conjugated System

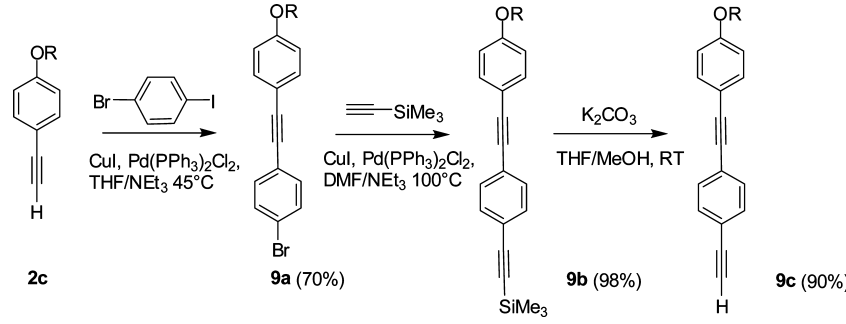

Scheme 3. Syntheses of the Chalcone-Acetylide Moieties

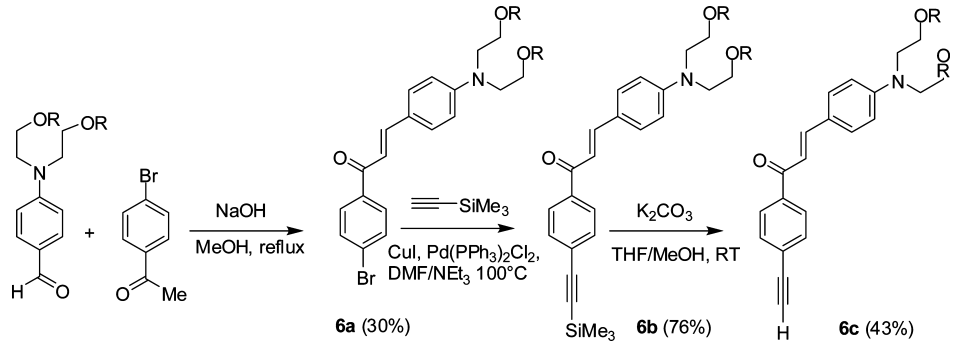

ethoxy)ethylmethylsulfonate or 1-chloro-2-(2-(2-methoxyethoxy)ethoxy)ethane. The first synthons featuring phenylenethynyl moieties **1**−**5c** and **8c** were obtained in two steps (Scheme 1): first, a Sonogashira cross-coupling reaction with trimethylsilylacetylene using standard experimental conditions (THF/triethylamine at 45 °C for the iodo derivatives and DMF/triethylamine at 100 °C for the bromo ones) yielded **1**−**5b** and **8b** in good yield. The trimethylsilyl protecting group (TMS) was further cleaved with potassium carbonate. Extension of conjugation by the incorporation of an additional phenylenethynylene unit (**9c**) was performed by two subsequent Sonogashira cross-coupling reactions with (i) bromo-iodobenzene and (ii) TMS-acetylene followed by deprotection of the TMS moieties (Scheme 2). Finally, chalcone derivative **6a** was prepared by the condensation of dialkylaminobenzaldehyde and 4-bromoacetophenone following literature procedures. Addition of the ethynylene fragment in **6c** was then realized as described above for the other systems (Scheme 3). Cross-coupling of all of these donor-π-conjugated-acetylide synthons (**1**−**6c** and **8**−**9c**) with dimethyl-4-iodo-pyridine-2,6-dicarboxylate, whose large-scale synthesis has been previously reported,[53] gave **1**−**6d** and **8**−**9d** in moderated to good yields after purification by

(53) Picot, A.; Feuvrie, C.; Barsu, C.; Malvolti, F.; Le Guennic, G.; Le Bozec, H.; Andraud, C.; Toupet, L.; Maury, O. *Tetrahedron* **2008**, *64*, 399–411.

Scheme 4. Ligands Synthesis

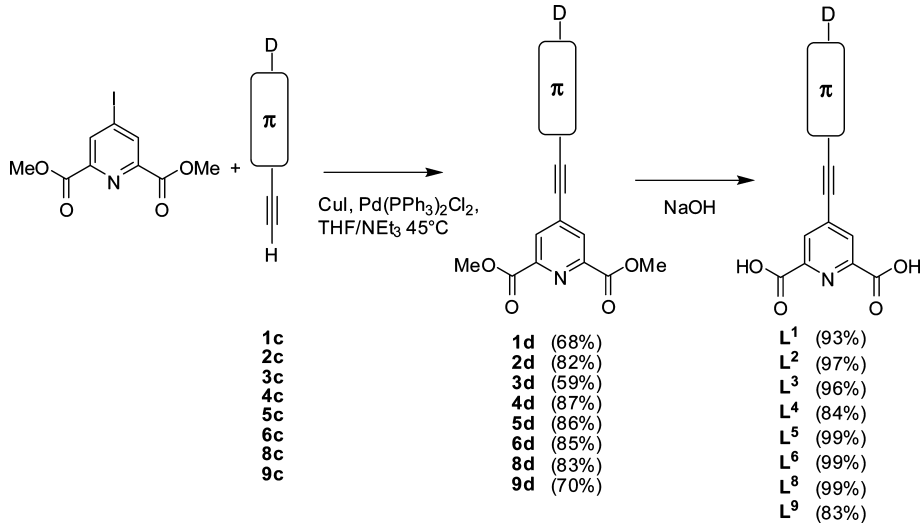

Scheme 5. Preparation of $\mathbf{L}^7$

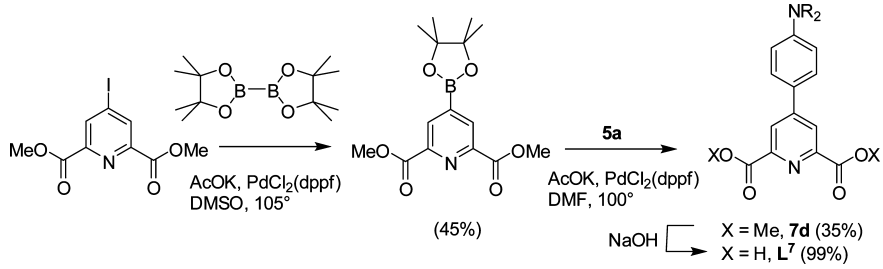

column chromatography (Scheme 4). Final saponification of the ester moieties by sodium hydroxide led to the formation of the tridendate ligands $\mathbf{L^1}-\mathbf{L^6}$ and $\mathbf{L^8}-\mathbf{L^9}$ in excellent yields. The synthesis of $\mathbf{L}^7$, featuring a simple phenyl link between donor and acceptor fragments, involved a Suzuki cross-coupling between dimethyl-4-(pinacolatoboronic ester)-2,6-dicarboxylate and **5a** catalyzed with $PdCl_2$(dppf) (dppf = diphenylferrocenyl-phosphine) in DMF at 100 °C followed by saponification of the ester moieties (Scheme 5). It is important to note that all of the syntheses were carried out on a large scale (few hundreds of milligrams to several grams) and that the intermediates as well as the ligands are isolated as sticky oils (except for $\mathbf{L^8}$ and $\mathbf{L^9}$), which makes the synthesis uncomfortable. All of the molecules were fully characterized by ^{1}H NMR, ^{13}C NMR, and mass spectrometry. In addition, final ligands $\mathbf{L^1}-\mathbf{L^9}$ give satisfactory microanalyses. Their photophysical properties were thoroughly described in the preceding paper. Finally, the corresponding europium complexes $[A]_3[Eu\mathbf{L^{1-9}}_3]$ (A stands for NBu_4, Chart 1) were prepared in water by mixing 3 equiv of ligands with hydrated lanthanide chloride in the presence of NBu_4OH acting as base and counterion, followed by extraction with dichloromethane. The resulting complexes are isolated as oils (except for $\mathbf{L^8}$ and $\mathbf{L^9}$). ^{1}H and ^{13}C NMR spectra reveal only one set of signals in agreement with the 3-fold symmetry of the complexes, and the dipicolinate proton chemical shifts are in agreement with data reported in the literature.[54] In addition, all europium complexes present elemental analyses corresponding to the formation of dichloromethane solvate.

2. Photophysical Properties. All of the complexes present broad intense transitions in the UV/visible spectrum (Figure 1 and Table 1) assigned to intraligand CT transitions on the basis of time-dependent density functional theory calculations (vide part 1 paper). It is worth noting that the absorption bands of complexes $[A]_3[Eu\mathbf{L^1}_3]$ and $[A]_3[Eu\mathbf{L^2}_3]$ present a shoulder corresponding to the overlap between the local excited state and the CT transitions. As shown in part 1, increasing the strength of the donor from $-CH_2OR$, $-OR$, $-SR$, or $-NR_2$ results in a strong bathochromic shift of the CT band from 312 to 370 nm ($\Delta\lambda = 60$ nm, Table 1). On the other hand, lengthening the π-conjugated backbone in the series $[A]_3[Eu\mathbf{L^{2,8,9}}_3]$ featuring an alkoxy donor group induces a less-pronounced red-shift ($\Delta\lambda = 14$ nm) but a significant hyperchromic effect and broadening of the absorption band (Figure 1).[8,55,56] A similar effect is observed in the series $[A]_3[Eu\mathbf{L^{7,5,6}}_3]$ featuring dialkylamino donor group. In addition, $[A]_3[Eu\mathbf{L^6}_3]$ featuring dialkylaminochalcone moieties exhibits the most red-shifted transition centered at 427 nm. All complexes, except $[A]_3[Eu(\mathbf{L^6})_3]$, exhibit the classical emission profile of europium tris-dipicolinate, with a very intense hypersensitive $^5D_0 \rightarrow {}^7F_2$ transition (Figure 2).[47−49] The quantum yields vary from 5.9% to 43% and the lifetimes from 0.45 to 1.9 ms, depending on the nature

(54) Ouali, N.; Bocquet, B.; Rigault, S.; Morgantini, P.-Y.; Weber, J.; Piguet, C. *Inorg. Chem.* **2002**, *41*, 1436–1445.

(55) Nah, M.-K.; Cho, H.-G.; Kwon, H.-J.; Kim, Y.-J.; Park, C.; Kim, H. K.; Kang, J.-G. *J. Phys. Chem. A* **2006**, *110*, 10371–10374.

(56) Meier, H.; Gerold, J.; Kolshorn, H.; Mühling, B. *Chem.—Eur. J.* **2004**, *10*, 360–370.

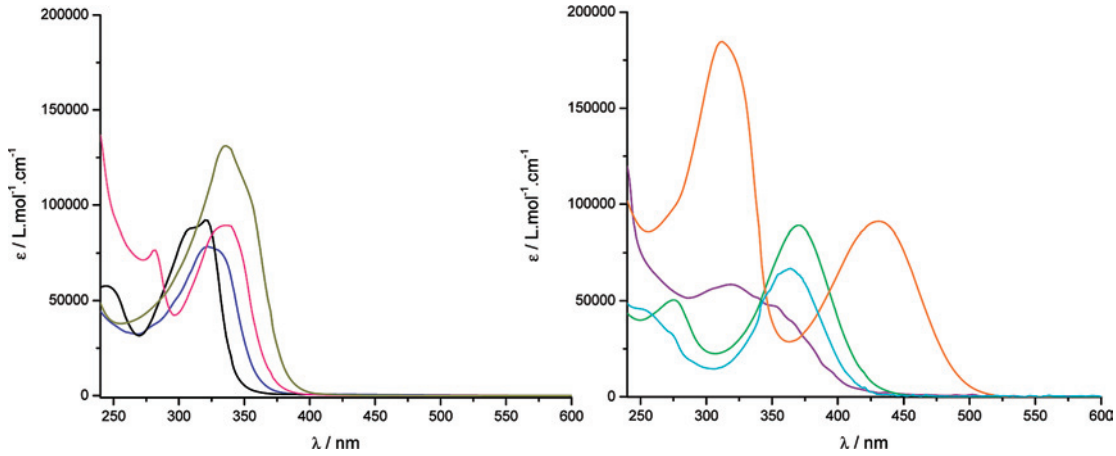

Figure 1. UV/visible absorption spectra in dichloromethane of $[A]_3[EuL^2_3]$ (black), $[A]_3[EuL^3_3]$ (blue), $[A]_3[EuL^8_3]$ (red), and $[A]_3[EuL^9_3]$ (green) (left) and $[A]_3[EuL^4_3]$ (purple), $[A]_3[EuL^5_3]$ (green), $[A]_3[EuL^6_3]$ (orange), and $[A]_3[EuL^7_3]$ (aqua) (right).

Table 1. Photophysical and Two-Photon Absorption Data in Dichloromethane Solution

	λ_{abs}^{max} (nm)	ε^{max} (L mol^{-1} cm^{-1})	λ_{em}^{max} (nm)	ϕ_L	τ_{Ln} (ms)	σ_2 (GM)	λ_{TPA} (nm)[a]
$[A]_3[EuL^1_3]$	312	61300	613	0.059	0.86		
$[A]_3[EuL^2_3]$	321	92000	613	0.15	1.90	14	700
$[A]_3[EuL^3_3]$	322	79000	613	0.43	1.42	53	700
$[A]_3[EuL^4_3]$	318	58500	613	0.27	1.81	96	740
$[A]_3[EuL^5_3]$	370	89200	613	0.070	0.85	775	740
$[A]_3[EuL^6_3]$	427	94000	565	0.070[b]		173	840
$[A]_3[EuL^7_3]$	364	63600	613	0.28	1.75	193	730
$[A]_3[EuL^8_3]$	335	86000	613	0.090	0.90	110	700
$[A]_3[EuL^9_3]$	335	131000	613	0.036	0.45	218	700

[a] λ_{TPA} stated for the wavelength of which the maximum two-photon cross-section has been measured within the laser spectral range (700−900 nm). [b] Emission from the CT state.

of the antenna ligand (donor group and conjugation length; Table 1). Detailed studies of the luminescence properties of $[A]_3[Eu(L^{1-6})_3]$, reported in the part 1 paper, indicate that europium luminescence is sensitized directly from the CT state for these complexes.[57−59] In the part 1 paper, it was demonstrated that the global efficiency of the sensitization process (in terms of luminescence quantum yield) presents a maximum depending on (i) the relative position between the energy levels of the CT donating state and the europium $^5D_1$ and $^5D_0$ accepting states and (ii) the intrinsic antenna quantum yield. In addition, for a given alkoxy donor group, lengthening the conjugated pathway from phenylethynyl (L^2), naphtylenthynyl (L^8), and bis-phenylethynyl (L^9) results in a regular decrease of both quantum yield and lifetime. This tendency indicates a less efficient energy transfer to Eu^{III} that is in agreement with the presence of a residual CT broad emission band centered at 402 nm in the case of $[A]_3[Eu(L^9_3)]$ (Figure 2). It is worth noting that this new sensitization processes through the CT state allows for reaching high quantum yield efficiency (43% in the case of $[A]_3[Eu(L^2)_3]$). Finally, in the case of $[A]_3[Eu(L^6)_3]$, featuring the most red-shifted absorption band (Table 1), only the broad ligand-centered CT fluorescence is observed without any europium luminescence, as detailed in part 1 (Figure 3). This result can be explained by the too low energy level of the antenna ligand L^6 for the sensitization of europium.

3. Two-Photon Absorption Properties. The two-photon absorption cross-sections (σ_{TPA}) have been determined in dichloromethane solution using the two-photon excited fluorescence technique in the 700−900 nm wavelength range with a femtosecond Ti-Sapphire pulsed laser source, according to the experimental protocol described by Xu and Webb.[60] The quadratic dependence of the europium luminescence intensity versus incident laser power has been checked, and an example is depicted in the case of $[A]_3[EuL^5_3]$ (Figure 4). In that case, the experimental regression coefficient is estimated at about 1.8 (th: 2), indicating that, in the experimental laser power range, no saturation or photodegradation occurs and unambiguously confirming that the luminescence arises from a two-photon absorption process. The two-photon excitation spectra were calibrated using coumarin-307 as a standard[60] (see the Experimental Section for details). For all compounds, the two-photon excitation spectra match the wavelength-doubled scale single-photon one (Figures 5, 6, and 7 in the cases of $[A]_3[EuL^5_3]$, $[A]_3[EuL^9_3]$, and $[A]_3[EuL^6_3]$, respectively). This good correlation is in agreement with the two-photon selection rules and is characteristic for noncentrosymmetric derivatives such as, for example, the D_3 symmetric octupolar complexes described in the present study.[55,61−63] It indicates that the lowest excited state in energy, here a CT state, is one- and two-photon-allowed and confirms that the europium luminescence (except for $[A]_3[EuL^6_3]$) is induced by a two-photon antenna effect with a similar photophysical sensitiza-

(57) Werts, M. H. V.; Jukes, R. T. F.; Verhoeven, J. W. *Phys. Chem. Chem. Phys.* **2002**, *4*, 1542–1548.
(58) Yang, C.; Fu, L. M.; Wang, Y.; Zhang, J. P.; Wong, W. T.; Ai, X. C.; Qiao, Y. F.; Zou, B. S.; Gui, L. L. *Angew. Chem., Int. Ed.* **2004**, *43*, 5010–5013.
(59) Kim, Y. H.; Baek, N. S.; Kim, H. K. *ChemPhysChem* **2006**, *7*, 213–221.
(60) Xu, C.; Webb, W. W. *J. Opt. Soc. Am. B* **1996**, *13*, 481–491.
(61) Bhaskar, A.; Ramakrishna, G.; Lu, Z.; Twieg, R.; Hales, J. M.; Hagan, D. J.; Van Stryland, E.; Goodson, T., III. *J. Am. Chem. Soc.* **2006**, *128*, 11840–11849.
(62) Mazzucato, S.; Fortunati, I.; Scolaro, S.; Zerbetto, M.; Ferrante, C.; Signorini, R.; Bozio, R.; Locatelli, D.; Righetto, S.; Roberto, D.; Ugo, R.; Abbotto, A.; Archetti, G.; Beverina, L.; Ghezzi, S. *Phys. Chem. Chem. Phys.* **2007**, *9*, 2999–3005.
(63) Rumi, M.; Ehrlich, J. E.; Heikal, A. A.; Perry, J. W.; Barlow, S.; Hu, Z.; McCord-Maughon, D.; Parker, T. C.; Röckel, H.; Thayumanavan, S.; Marder, S. R.; Beljonne, D.; Brédas, J.-L. *J. Am. Chem. Soc.* **2000**, *122*, 9500–9510.

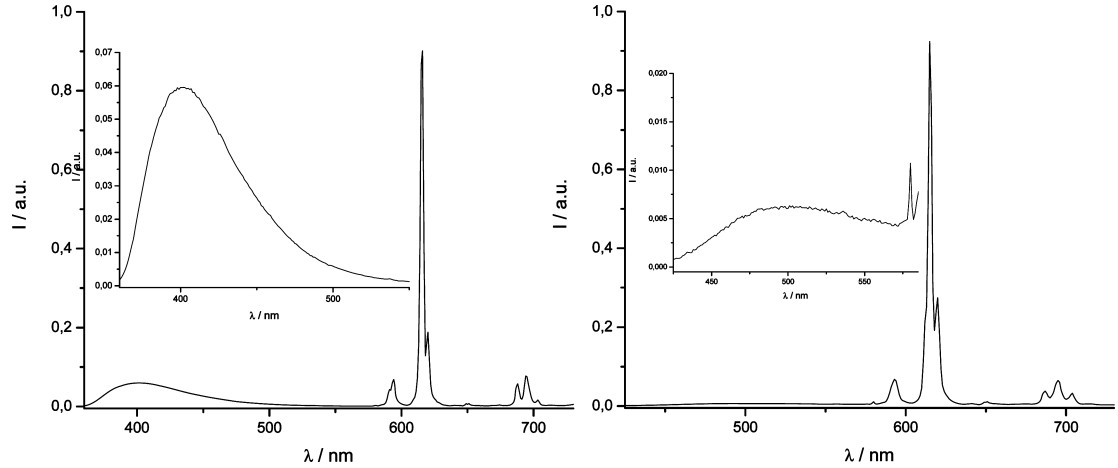

Figure 2. Room temperature emission spectra in DCM solution of $[A]_3[Eu(\mathbf{L}^9)_3]$, inset: emission of residual CT state zoom × 10 (λ_{exc}= 340nm) (left). Room temperature emission spectra in DCM solution of $[A]_3[Eu(\mathbf{L}^5)_3]$, inset: emission of residual CT state zoom × 100 (λ_{exc}= 340 nm) (right).

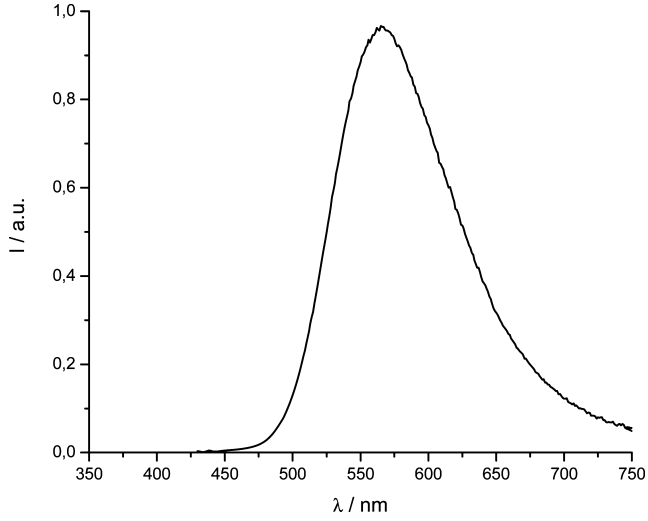

Figure 3. Room temperature emission spectrum in DCM solution of $[A]_3[Eu(\mathbf{L}^6)_3]$.

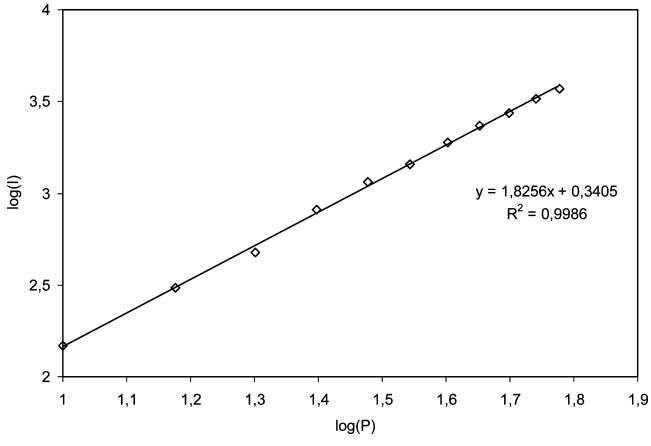

Figure 4. Plot of the europium emission intensity at 613 nm versus incident laser power for $[A]_3[Eu\mathbf{L}^5_3]$ (λ_{ex} = 800 nm) on a log/log scale. The fit of the experimental data is shown in black, and the corresponding equation and standard deviation are reported in the inset.

tion process, namely, two-photon absorption in the antenna CT state followed by a direct energy transfer to the metal ion (Scheme 6). In the particular case of $[A]_3[Eu\mathbf{L}^6_3]$, no europium sensitization occurs, so only the CT emission is observed upon one- or two-photon excitation (Scheme 6).

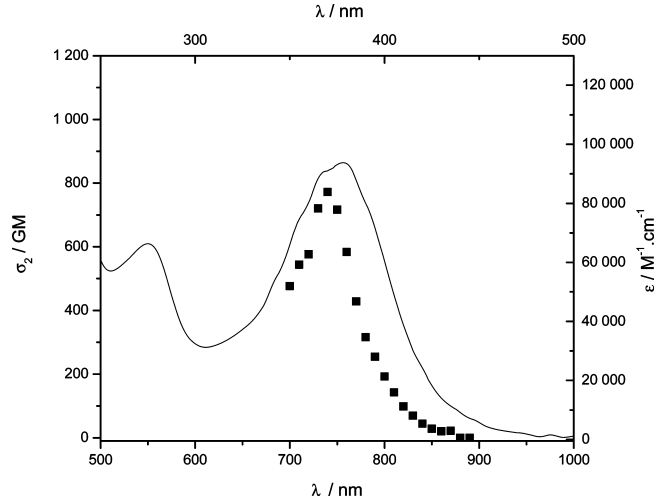

Figure 5. Two-photon excitation spectrum of $[A]_3[Eu\mathbf{L}^5_3]$ in dichloromethane solution (■, lower abscissa). Superimposed on this plot is the single-photon absorption spectrum in wavelength doubled scale (−, upper abscissa).

The maximal two-photon absorption cross-section (σ_2) and the maximal TPA wavelength (λ_{TPA}) are summarized in Table 1. In the cases of $[A]_3[Eu\mathbf{L}^2_3]$ and $[A]_3[Eu\mathbf{L}^3_3]$, featuring weak alkoxy or alkylthio donor groups, the maximal TPA wavelength is located out of the laser range, and only a weak tail corresponding to the red edge of the band is detected (Figure 8). Similarly, it was not possible to record any TPA excitation spectrum in the case of $[A]_3[Eu\mathbf{L}^1_3]$ in the 700−900 nm range because its absorption is located at too high an energy, and the remaining TPA cross-section in the experimental range was too low. Although increasing the length of the conjugated backbone with a naphtyl linker (in $[A]_3[Eu\mathbf{L}^8_3]$) should allow a red-shift of the TPA band, as is the case for the UV/visible absorption band, the TPA maximum remains out of the spectral range. However, at 700 nm, the two-photon cross-section is now about 110 GM, which is as high as other values found in the literature for other europium complexes.[43−46] When extending the conjugated backbone as for $[A]_3[Eu\mathbf{L}^9_3]$, the λ_{TPA} value is found to be at 700 nm, twice the single absorption wavelength of the shoulder at 354 nm (Figure 6) with a high TPA cross-section of 218 GM. The 2-fold increase of the σ_2 from

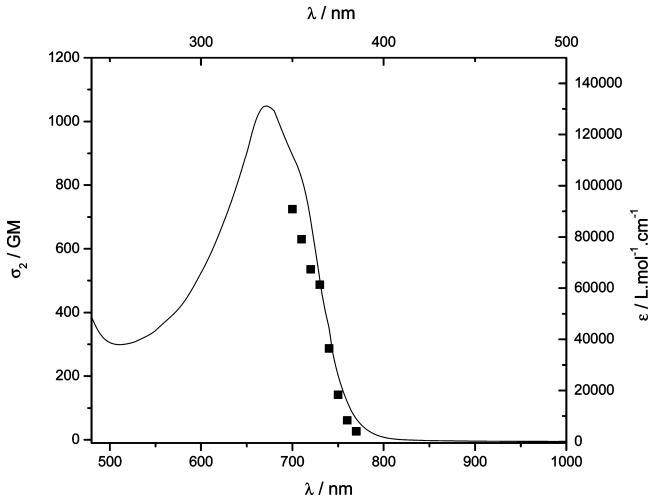

Figure 6. Two-photon excitation spectrum of $[A]_3[EuL^9_3]$ in dichloromethane solution (■, lower abscissa). Superimposed on this plot is the single-photon absorption spectrum in wavelength doubled scale (−, upper abscissa).

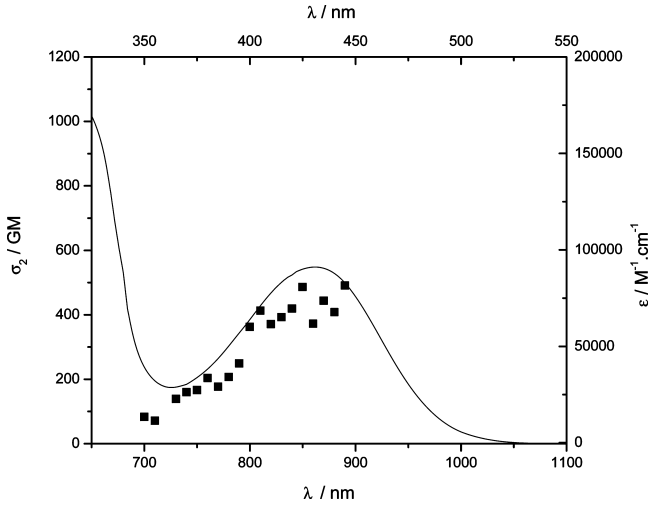

Figure 7. Two-photon excitation spectrum of $[A]_3[EuL^6_3]$ in dichloromethane solution (■, lower abscissa). Superimposed on this plot is the single-photon absorption spectrum in wavelength doubled scale (−, upper abscissa).

Scheme 6. Schematic Representation of the Two-Photon Excited Photophysical Process

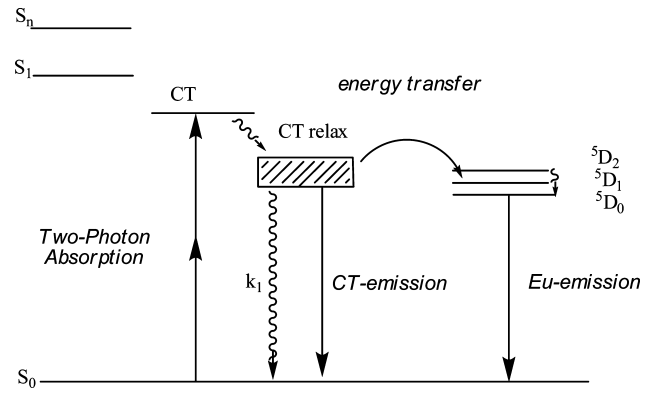

$[A]_3[EuL^8_3]$ to $[A]_3[EuL^9_3]$ can be related to the hyperchromic effect observed in one-photon absorption spectra, and a similar enhancement of σ_2 by lengthening the π-squeleton are classically observed for organic chromophores.[55,61,63]

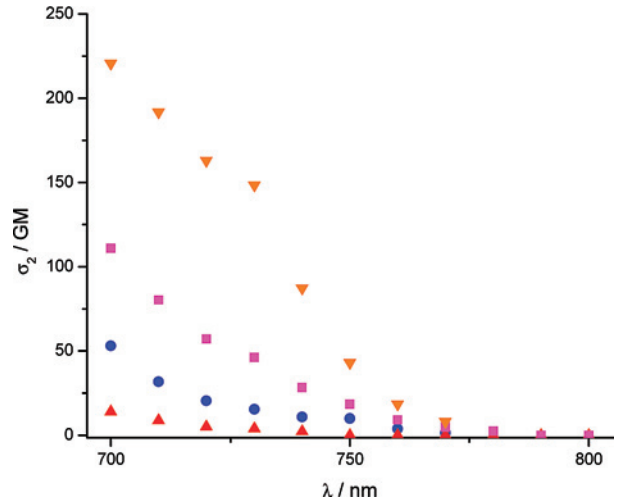

Figure 8. Two-photon excitation spectra of $[A]_3[Eu(L^2)_3]$ (red ▲), $[A]_3[Eu(L^3)_3]$ (blue ●), $[A]_3[Eu(L^8)_3]$ (purple ■), and $[A]_3[Eu(L^9)_3]$ (orange ▼) in dichloromethane solution.

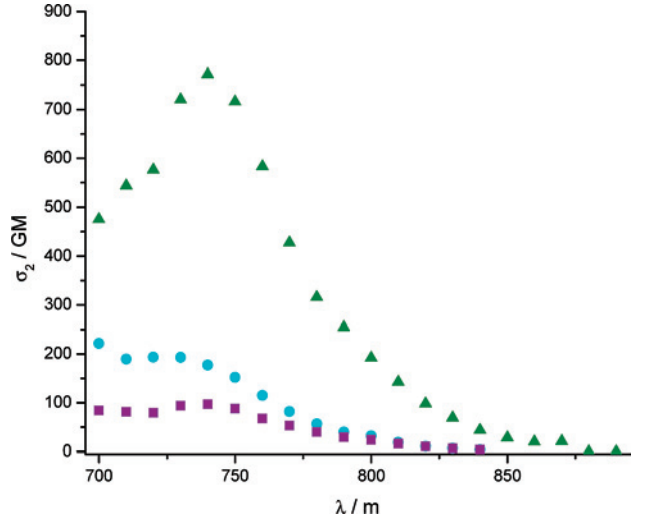

Figure 9. Two-photon excitation spectra of $[A]_3[Eu(L^4)_3]$ (purple ■), $[A]_3[Eu(L^5)_3]$ (green ▲), and $[A]_3[Eu(L^7)_3]$ (aqua ●) in dichloromethane solution.

Finally, replacing the alkoxy by a stronger amino donor group induces a strong enhancement of the two-photon cross-section accompanied by a large red-shift of the maximum TPA wavelength (775 GM at 740 nm), which is the highest value ever reported for a Eu complexes.[43−46] In this series, reducing the conjugation either by shortening or by twisting the π skeleton in $[A]_3[EuL^7_3]$ and $[A]_3[EuL^4_3]$, respectively, results in a significant decrease of σ_2 (193 and 96 GM, respectively; Figure 9).

Furthermore, in the case of the amino-donor-containing complexes, the two-photon cross-section remains significant in the spectral range where the nonlinear microscopy imaging experiments are generally performed (750−800 nm). For instance, at 780 nm, a TPA cross-section of about 315 GM is obtained for $[A]_3[EuL^5_3]$, more than 1 order of magnitude higher than that of our benchmark complex $Na_3[Eu(L^{2G})_3]$ (σ_2 (760) = 19 GM and σ_2 (780) = 5 GM).[52] Keeping in mind that most of the intensity of the Eu emission is concentrated in the sharp hypersensitive $^5D_0 \rightarrow {}^7F_2$ band (70% of the emission area), these complexes are interesting

candidates for two-photon imaging applications. Interestingly, the remarkable σ_2 value reached in the case of $[A]_3[Eu\mathbf{L}^5{}_3]$ (775 GM at 740 nm) can be considered close to the upper limit that can be reached for this family of complexes. Indeed, although higher σ_2 values should be expected by further extension of the π system, for example, the resulting lower gap between the antenna ground state and the Eu excited state will prohibit any energy transfer to the metal as in $[A]_3[Eu(\mathbf{L}^6)_3]$. This upper limit depends of course on the nature of the lanthanide and on its sensitization process. As a consequence, a higher σ_2 could be obtained using more conjugated ligands, for NIR-emitting lanthanides (Yb, Nd, or Er), whereas lower limit values are expected with weakly conjugated systems for Tb or Dy, for which accepting excited states lie at higher energy.

Conclusion

In conclusion, we designed a new versatile family of chromophore-based ligands able to induce europium emission by a two-photon antenna effect. Tuning the strength of the donor as well as the length of the π-conjugated backbone allows optimization of the TPA cross-section, 775 GM at 740 nm for $[A]_3[Eu\mathbf{L}^5{}_3]$, and a shift of the maximal TPA wavelength to the red. In the spectral region of interest (750−800 nm), this latter compound conserves a very significant TPA cross-section. These results emphasize the high potentialities of this class of compounds: (i) the high σ_2 values are promising for the sensitization of NIR emitters such as ytterbium and neodymium, and (ii) their stability in water is of prime importance for the further design of a new family of bioprobes with enhanced water solubility. These results combined with two-photon excited time-gated spectroscopy experiments recently demonstrated[51] open the way to an improved biological imaging technique: *biphotonic time-gated microscopy*, combining the advantage of both lanthanides and two-photon microscopy.

Experimental Section

Luminescence Measurements: Luminescence. The luminescence spectra were measured using a Horiba-Jobin Yvon Fluorolog-3 spectrofluorimeter (see the preceding article for details). Phosphorescence lifetimes (>30 μs) were obtained by pulsed excitation using an FL-1040 UP xenon lamp. Luminescence decay curves were fitted by least-squares analysis using Origin. Fluorescence quantum yields, Q, were measured in a diluted solution with an optical density lower than 0.1 using the following equation: $Q_x/Q_r = [A_r(\lambda)/A_x(\lambda)][n_x^2/n_r^2][D_x/D_r]$, where A is the absorbance at the excitation wavelength (λ), n is the refractive index, and D is the integrated luminescence intensity. The "r" and "x" stand for reference and sample. Here, references are the quinine bisulfate in 1 N sulfuric acid in aqueous solution ($Q_r = 0.546$)[64] and $Ru(bpy)_3$ 2Cl complexes in a water solution ($Q_r = 0.028$)[65] for each complex.

Two-Photon Excited Luminescence Measurements. The TPA cross-section spectra were obtained by up-conversion fluorescence using a Ti:sapphire femtosecond laser in the range 700−900 nm. The excitation beam (5 mm diameter) is focalized with a lens (focal length 10 cm) at the middle of the fluorescence cell (10 mm). The fluorescence, collected at 90° to the excitation beam, was focused into an optical fiber (diameter 600 μm) connected to an Ocean Optics S2000 spectrometer. The incident beam intensity was adjusted to 50 mW in order to ensure an intensity-squared dependence of the fluorescence over the whole spectral range. The detector integration time was fixed to 1 s. Calibration of the spectra was performed by comparison with the published 700−900 nm Coumarin-307 two-photon absorption spectrum[60] (Coumarin-307 quantum yield 0.56 in ethanol). The measurements were done at room temperature in dihloromethane and at a concentration of 10^{-4} M.

General Procedure. NMR spectra (^{1}H and ^{13}C) were recorded at room temperature on a BRUKER AC 200 operating at 200.13 and 50.32 MHz for ^{1}H and ^{13}C, respectively. Data are listed in parts per million (ppm) and are reported relative to tetramethylsilane (^{1}H and ^{13}C); residual solvent peaks of the deuterated solvents were used as an internal standard. UV/vis absorption measurements were recorded on a JASCO V550 absorption spectrometer. Low-resolution mass spectrometry was carried out on an Agilent 1100 Series LC/MSD apparatus. High-resolution mass spectrometry measurements and elemental analyses were performed at the Service Central d'Analyze du CNRS (Vernaison, France).

General Procedure for Sonogashira Cross-Coupling Reactions. In a 100 mL Schlenk flask, dimethyl-4-iodopyridine-2,6-dicarboxylate (1 equiv) was dissolved in a mixture a THF and triethylamine (15 mL/15 mL). The solution was thoroughly degassed by argon bubbling for 20 min and an acetylene derivative, copper iodide (0.2 equiv), and $(Ph_3P)PdCl_2$ (0.l equiv) were added under a flux of argon. The reaction was stirred at 40 °C for 14 h. The solution was evaporated under a vacuum, and the resulting oil was dissolved in ethylacetate and extracted with a NH_4Cl aqueous solution and with brine. The crude was purified by column chromatography on silica.

1d. Transparent oil (68%) from **1c** (835 g), chromatography conditions: ethyl acetate. ^{1}H NMR (200.13 MHz, $CDCl_3$): δ 8.28 (s, 2H), 7.59 (d, ^3J = 8.1 Hz, 2H), 7.32 (d, ^3J = 8.1 Hz, 2H), 4.53 (s, 2H), 3.96 (s, 6H), 3.60 (m, 10H), 3.50 (m, 2H), 3.30 (s, 3H). ^{13}C NMR (50.332 MHz, $CDCl_3$): 164.81, 148.57, 140.70, 134.60, 132.23, 129.71, 127.73, 120.50, 97.03, 85.45, 72.73, 72.06, 70.75, 70.66, 69.94, 59.12, 53.39. EI-MS: $[M + H]^+$, 472; $[M + Na]^+$, 494.

2d. Transparent oil (84%) from **2c** (1.84 g), chromatography conditions: dichloromethane/ethyl acetate (9/1). ^{1}H NMR (200.13 MHz, $CDCl_3$): δ 8.29 (s, 2H), 7.43 (d, ^3J = 8.8 Hz, 2H), 6.87 (d, ^3J = 8.8 Hz, 2H), 4.13 (t, ^3J = 4.9 Hz, 2H), 3.99 (s, 6H), 3.86 (t, ^3J = 4.5 Hz, 2H), 3.64 (m, 6H), 3.52 (m, 2H), 3.34 (s, 3H). ^{13}C NMR (50.332 MHz, $CDCl_3$): δ 165.0, 160.4, 148.6, 135.1, 134.0, 129.7, 115.2, 113.7, 97.7, 84.9, 72.2, 71.1, 70.9, 70.8, 69.8, 67.8, 59.3, 53.5. EI-MS: $[M + H]^+$, 458; $[M + Na]^+$, 480. Elem anal. calcd for $C_{24}H_{27}NO_8$: C, 63.01; H, 5.95; N, 3.06. Found: C, 62.76; H, 5.84; N, 2.92.

3d. Transparent oil (59%) from **3c** (620 mg), chromatography conditions: ethyl acetate. ^{1}H NMR (200.13 MHz, $CDCl_3$): δ 8.28 (s, 2H), 7.41 (d, ^3J = 8.3 Hz, 2H), 7.27 (d, ^3J = 8.4 Hz, 2H), 3..98 (s, 6H), 3.86 (t, ^3J = 4.5 Hz, 2H), 3.59 (m, 8H), 3.50 (m, 2H), 3.32 (s, 3H), 3.13 (t, ^3J = 6.8 Hz, 2H). ^{13}C NMR (50.332 MHz, $CDCl_3$): δ 164.8, 148.6, 139.9, 134.6, 133.5, 129.7, 127.8, 118.3, 96.9, 85.9, 72.1, 70.7, 70.7, 69.8, 59.2, 53.4, 32.2. EI-MS: $[M + Na]^+$, 474; $[M + Na]^+$, 496.

4d. Orange oil (87%) from **4c** (300 mg), chromatography conditions: chloroform/diethylether (3/1). ^{1}H NMR (200.13 MHz, $CDCl_3$): δ 8.28 (s, 2H), 7.19 (s, 2H), 3.99 (s, 6H), 3.50 (m, 20H),

(64) Demas, J. N.; Crosby, G. A. *J. Phys. Chem.* **1971**, *75*, 991–1024.
(65) Nakamaru, K. *Bull. Chem. Soc. Jpn.* **1982**, *55*, 2697–2705.

3.33 (s, 6H), 3.25 (t, ^3J = 5.8 Hz, 4H), 2.26 (s, 6H). ^{13}C NMR (50.332 MHz, $CDCl_3$): δ 165.0, 150.2, 148.6, 138.2, 135.1, 132.7, 129.7, 117.4, 97.9, 85.0, 72.1, 70.8, 70.7, 70.5, 59.2, 53.7, 53.4, 19.3. EI-MS: $[M + H]^+$, 631; $[M + Na]^+$, 653.

5d. Orange oil (86%) from **5c** (370 mg), chromatography conditions: ethyl acetate. ^{1}H NMR (200.13 MHz, $CDCl_3$): δ 8.19 (s, 2H), 7.21 (d, ^3J = 8.7 Hz, 2H), 6.61 (d, ^3J = 8.9 Hz, 2H), 3.93 (s, 6H), 3.46 (m, 24H), 3.28 (s, 6H). ^{13}C NMR (50.332 MHz, $CDCl_3$): δ 164.9, 150.0, 148.2, 135.4, 133.7, 111.5, 107.4, 95.6, 84.5, 71.9, 70.7, 70.5, 68.3, 59.0, 53.1, 50.8. Elem anal. calcd for $C_{31}H_{42}N_2O_{10}$: C, 61.78; H, 7.02; N, 4.65. Found: C, 61.44; H, 6.96; N, 4.62.

6d. Orange solid (85%) from **6c** (115 mg), chromatography conditions: ethyl acetate/methanol (95/5). ^{1}H NMR (200.13 MHz, $CDCl_3$): δ 8.38 (s, 2H), 8.02 (d, ^3J = 8.2 Hz, 2H), 7.78 (d, ^3J = 15.4 Hz, 1H), 7.67 (d, ^3J = 8.2 Hz, 2H), 7.29 (d, ^3J = 15.4 Hz, 1H), 6.71 (d, ^3J = 8.8 Hz, 2H), 4.03 (s, 6H), 3.56 (m, 32H), 3.35 (s, 6H). ^{13}C NMR (50.332 MHz, $CDCl_3$): δ 189.36, 164.63, 150.25, 148.55, 146.42, 139.75, 134.03, 132.17, 130.79, 129.68, 128.43, 124.88, 122.43, 116.19, 111.71, 96.02, 87.52, 71.92, 70.76, 70.61, 70.51, 68.38, 50.02, 53.34, 50.94.

8d. White oil (83%) from **8c** (1.82 g), chromatography conditions: ethyl acetate. ^{1}H NMR (200.13 MHz, $CDCl_3$): δ 8.29 (s, 2H), 7.95 (s, 1H), 7.64 (m, 2H), 7.47 (d, ^3J = 8.3 Hz, 1H), 7.13 (m, 2H), 4.19 (m, 2H), 3.97 (s, 6H), 3.86 (m, 2H), 3.63 (m, 6H), 3.50 (m, 2H), 3.30 (s, 3H). ^{13}C NMR (50.332 MHz, $CDCl_3$): δ 164.7, 158.2, 148.4, 134.9, 134.6, 132.5, 129.6, 129.5, 128.6, 128.3, 127.2, 120.1, 116.1, 106.8, 97.9, 85.3, 71.9, 70.9, 70.7, 70.6, 69.6, 67.5, 59.0, 53.3. EI-MS: $[M + H]^+$, 508; $[M + Na]^+$, 530.

9d. White solid (70%) from **9c** (310 mg), chromatography conditions: dichloromethane/diethylether (9/1) to dichloromethane/diethylether (4/1). ^{1}H NMR (200.13 MHz, $CDCl_3$): δ 8.26 (s, 2H), 7.37 (m, 6H), 6.82 (d, ^3J = 8.9 Hz, 2H), 4.07 (m, 2H), 3.95 (s, 6H), 3.78 (t, ^3J = 5.0 Hz, 2H), 3.57 (m, 6H), 3.47 (m, 2H), 3.30 (s, 3H). ^{13}C NMR (50.332 MHz, $CDCl_3$): δ 164.6, 159.2, 148.4, 134.2, 133.1, 132.0, 131.5, 129.5, 129.3, 120.5, 114.9, 114.7, 96.6, 92.5, 87.6, 86.9, 71.9, 70.8, 70.6, 70.5, 69.6, 67.5, 59.0, 53.3. EI-MS: $[M + H]^+$, 558; $[M + Na]^+$, 580.

General Procedure for the Ligand Deprotection. In a 100 mL round-bottom flask, the ligand diester precursor **1**−**10d** was dissolved in 15 mL of methanol; a solution of NaOH (4−5 equiv) in water (20 mL) wad added, and the reaction was stirred at room temperature for 1 h. The methanol was evaporated; the water phase was extended to 100 mL, and the aqueous phase was extracted with ethyl acetate (two times). The water was acidified with HCl (10%) until the pH was 1−2, and the aqueous phase was extracted three times with dichloromethane. The organic phases were regrouped and dried over sodium sulfate. After evaporation of the organic solvents, the white solid was dried at room temperature under a vacuum for 1 h.

L^1. White solid (93%). ^{1}H NMR (200.13 MHz, $CDCl_3$): δ 10.00 (bs, 2H), 8.27 (s, 2H), 7.31 (d, ^3J = 8.0 Hz, 2H), 7.19 (d, ^3J = 8.0 Hz, 2H), 4.49 (s, 2H), 3.66 (m, 8H), 3.55 (m, 2H), 3.45 (m, 2H), 3.25 (s, 3H). ^{13}C NMR (50.332 MHz, $CDCl_3$): 164.1, 146.2, 140.0, 135.7, 132.1, 129.2, 127.7, 120.2, 97.6, 85.6, 72.7, 71.7, 70.6, 70.5, 70.4, 70.3, 70.0, 58.8. Elem anal. calcd for $C_{23}H_{25}NO_8 \cdot 2H_2O$: C, 57.61; H, 6.10; N, 2.92. Found: C, 57.86; H, 5.35; N, 2.89.

L^2. White solid (97%). ^{1}H NMR (200.13 MHz, $CDCl_3$): δ 8.14 (s, 2H), 7.23 (d, ^3J = 8.7 Hz, 2H), 6.60 (d, ^3J = 8.7 Hz, 2H), 3.99 (m, 2H), 3.88 (m, 2H), 3.78 (s, 4H), 3.64 (m, 2H), 3.52 (m, 2H), 3.22 (s, 3H). ^{13}C NMR (50.332 MHz, $CDCl_3$): δ 164.28, 159.7, 146.1, 136.2, 134.1, 129.1, 114.6, 113.7, 98.5, 85.3, 71.9, 70.9, 70.6, 70.0, 67.4, 59.0. EI-MS: $[M + H]^+$, 430; $[M + Na]^+$, 452. Elem anal. calcd for $C_{22}H_{23}NO_8$: C, 61.53; H, 5.40; N, 3.26. Found: C, 61.57; H, 5.35; N, 3.13.

L^3. White solid (96%). ^{1}H NMR (200.13 MHz, $CDCl_3$): δ 9.83 (b, 2H), 8.31 (s, 2H), 7.35 (d, ^3J = 7.7 Hz, 2H), 7.17 (d, ^3J = 7.8 Hz, 2H), 3.66 (m, 8H), 3.57 (m, 2H), 3.35 (s, 3H), 3.11 (t, ^3J = 6.3 Hz, 2H). ^{13}C NMR (50.332 MHz, $CDCl_3$): 164.53, 146.48, 140.21, 135.89, 132.51, 129.48, 127.11, 117.79, 98.06, 85.73, 71.83, 70.49, 70.44, 70.38, 69.45, 58.93, 31.91. EI-MS: $[M + Na]^+$, 446 (446); $[M + Na]^+$, 468 (468). Elem anal. calcd for $C_{22}H_{23}NO_7S \cdot H_2O$: C, 57.01; H, 5.44; N, 3.02. Found: C, 56.89; H, 5.47; N, 2.84.

L^4. Orange solid (84%). ^{1}H NMR (200.13 MHz, $CDCl_3$): δ 8.99 (b, 2H), 8.29 (s, 2H), 6.99 (s, 2H), 3.50 (m, 20H), 3.29 (m, 10H), 2.21 (s, 6H). ^{13}C NMR (50.332 MHz, $CDCl_3$): 164.33, 149.99, 146.37, 137.62, 136.13, 132.59, 129.16, 117.03, 98.49, 85.37, 71.85, 70.42, 70.29, 58.89, 53.37, 18.99. Elem anal. calcd for $C_{31}H_{42}N_2O_{10} \cdot H_2O$: C, 59.99; H, 7.15; N, 4.51. Found: C, 58.98; H, 6.91; N, 4.30.

L^5. Orange solid (99%). ^{1}H NMR (200.13 MHz, $CDCl_3$): δ 8.20 (s, 2H), 7.12 (d, ^3J = 8.5 Hz, 2H), 6.48 (d, ^3J = 8.5 Hz, 2H), 3.49 (m, 24H), 3.30 (s, 6H). ^{13}C NMR (50.332 MHz, $CDCl_3$): δ 164.4, 149.0, 146.1, 136.8, 133.7, 111.6, 107.4, 100.8, 85.0, 71.8, 70.6, 70.6, 70.4, 68.3, 58.9, 50.5. EI-MS: $[M + H]^+$, 575; $[M + Na]^+$, 597. Elem anal. calcd for $C_{29}H_{38}N_2O_{10} \cdot H_2O$: C, 58.77; H, 6.80; N, 4.73. Found: C, 58.74; H, 6.80; N, 4.58.

L^6. Orange solid (99%). ^{1}H NMR (200.13 MHz, $CDCl_3$): δ 8.33 (s, 2H), 7.92 (d, ^3J = 7.4 Hz, 2H), 7.71 (d, ^3J = 15.0 Hz, 1H), 7.53 (d, ^3J = 7.4 Hz, 2H), 7.38 (d, ^3J = 7.4 Hz, 2H), 7.21 (d, ^3J = 15.0 Hz, 1H), 6.61 (d, ^3J = 7.4 Hz, 2H), 3.60 (m, 32H), 3.33 (s, 6H). ^{13}C NMR (50.332 MHz, $CDCl_3$): δ 189.12, 164.43, 150.22, 146.90, 146.51, 139.44, 135.03, 132.23, 130.80, 129.41, 128.40, 124.76, 122.44, 115.81, 111.70, 96.69, 87.58, 71.87, 70.58, 70.53, 70.42, 68.40, 58.98, 50.75. EI-MS: $[M + H]^+$, 793; $[M + Na]^+$, 815. Elem anal. calcd for $C_{42}H_{52}N_2O_{13} \cdot 2H_2O$: C, 60.86; H, 6.81; N, 3.38. Found: C, 60.03; H, 6.74; N, 3.44.

L^7. Orange-yellow solid (99%). ^{1}H NMR (200.13 MHz, $(CD_3)_2CO$): δ 8.25 (b, 2H), 7.82 (b, 2H), 6.94 (b, 2H), 3.58 (m, 24H), 3.26 (s, 6H). ^{13}C NMR (50.332 MHz, $(CD_3)_2CO$): δ 164.2, 152.0, 150.3, 147.1, 128.2, 122.5, 121.6, 112.3, 71.8, 70.5, 70.4, 70.3, 68.4, 57.9, 50.8. Elem anal. calcd for $C_{27}H_{38}N_2O_{10} \cdot H_2O$: C, 57.03; H, 7.09; N, 4.93. Found: C, 56.51; H, 7.08; N, 4.54.

L^8. White solid (96%). ^{1}H NMR (200.13 MHz, $CDCl_3$): δ 7.78 (s, 2H), 7.74 (s, 1H), 7.49 (s, 2H), 7.38 (d, ^3J = 9.2 Hz, 1H), 7.02 (dd, ^3J = 9.2 Hz, 1H), 6.76 (s, 1H), 4.21 (m, 2H), 3.96 (m, 2H), 3.79 (m, 4H), 3.63 (m, 2H), 3.54 (m, 2H), 3.25 (s, 3H). ^{13}C NMR (50.332 MHz, $CDCl_3$): δ 164.1, 157.5, 145.4, 134.9, 134.3, 132.6, 129.6, 129.2, 128.3, 128.0, 127.1, 119.7, 116.6, 106.0, 98.4, 85.1, 71.6, 70.7, 70.3, 69.9, 67.0, 58.7. Elem anal. calcd for $C_{26}H_{25}NO_8 \cdot H_2O$: C, 62.77; H, 5.47; N, 2.82. Found: C, 63.10; H, 5.28; N, 2.73.

L^9. White solid (83%).^{1}H NMR (200.13 MHz, $CDCl_3$): δ 8.22 (s, 2H), 7.28 (m, 4H), 7.19 (d, ^3J = 8.6 Hz, 2H), 6.59 (d, ^3J = 8.6 Hz, 2H), 4.02 (m, 2H), 3.92 (m, 2H), 3.83 (m, 4H), 3.68 (m, 2H), 3.55 (m, 2H), 3.26 (s, 3H). ^{13}C NMR (50.332 MHz, $CDCl_3$): δ 164.24, 158.48, 146.00, 135.43, 132.78, 131.88, 131.21, 128.94, 125.08, 120.23, 115.10, 114.05, 97.21, 91.95, 88.59, 87.05, 71.68, 70.73, 70.21, 70.13, 69.86, 66.86, 58.77. EI-MS: $[M + H]^+$, 530; $[M + Na]^+$, 552. Elem anal. calcd for $C_{30}H_{27}NO_8.H_2O$: C, 65.81; H, 5.34; N, 2.56. Found: C, 66.03; H, 5.09; N, 2.51.

General Procedure for the Synthesis of the Complexes. In a 100 mL round-bottom flask, **L^i** (i = 1−9, 3 equiv) and tetrabutylammonium hydroxide (40% in methanol, 6 equiv) were dissolved

in water (15 mL), and $EuCl_3 \cdot 6H_2O$ (1.05 equiv) was added. The solution was stirred at room temperature for 1 h. This aqueous mixture was extracted with dichloromethane (5 × 100 mL). The organic phases were combined, concentrated up to 40 mL, washed several times with water (5 × 100 mL), dried over magnesium sulfate, and evaporated under a vacuum. The products were obtained as hygroscopic light yellow or orange oils.

$[NBu_4]_3[Eu(L^1)_3]$. Colorless oil, yield: 67%. ^{1}H NMR (200.13 MHz, $CDCl_3$): δ 7.17 (b, 2H), 6.99 (b, 2H), 5.10 (b, 2H), 4.46 (b, 2H), 3.30 (m, 23H), 1.73 (b, 8H), 1.48 (b, 8H), 1.05 (b, 12H). Elem anal. calcd for $C_{117}H_{177}N_6O_{24}Eu \cdot 7CH_2Cl_2$: C, 53.23; H, 6.83; N, 3.00. Found: C, 53.61; H, 6.74; N, 2.93.

$[Bu_4N]_3[EuL^2_3]$. Light yellow oil, yield: 49%. ^{1}H NMR (200.13 MHz, $CDCl_3$): 6.89 (d, ^3J = 8.7 Hz, 6H), 6.65 (d, ^3J = 8.7 Hz, 6H), 5.56 (m, 24H), 4.95 (s, 6H), 3.98 (m, 6H), 3.75 (m, 18H), 3.57 (m, 6H), 3.44 (m, 6H), 3.29 (s, 9H), 2.88 (m, 24H), 2.00 (m, 24H), 1.11 (t, ^3J = 6.9 Hz, 36H). Elem anal. calcd for $C_{114}H_{171}N_6O_{24}Eu \cdot CH_2Cl_2$: C, 61.48; H, 7.76; N, 3.16. Found: C, 61.80; H, 8.05; N, 3.79.

$[Bu_4N]_3[Eu(L^3)_3]$. Yellow oil, yield: 67%. ^{1}H NMR (200.13 MHz, $CDCl_3$): δ 7.09 (d, ^3J = 8.0 Hz, 6H), 6.92 (d, ^3J = 7.9 Hz, 6H), 5.30 (b, 6H), 4.78 (m, 24H), 3.49 (m, 24H), 3.28 (s, 9H), 3.01 (t, ^3J = 6.6 Hz, 6H), 2.43 (b, 24H), 1.76 (b, 24H), 1.00 (b, 36H). ^{13}C NMR (50.332 MHz, $CDCl_3$): 165.78, 143.32, 141.68, 138.61, 132.78, 127.45, 117.77, 95.83, 85.12, 80.95, 71.85, 70.51, 70.40, 69.62, 60.33, 58.98, 32.32, 24.94, 20.23, 13.94. Elem anal. calcd for $C_{114}H_{171}N_6O_{21}S_3Eu \cdot 3CH_2Cl_2$: C, 57.02; H, 7.24; N, 3.41. Found: C, 57.38; H, 8.03; N, 3.28.

$[Bu_4N]_3[Eu(L^4)_3]$. Orange oil, yield: 76%. ^{1}H NMR (200.13 MHz, CD_3OD): δ 6.61 (s, 6H), 4.15 (bs, 6H), 3.45 (m, 84H), 3.21 (s, 18H), 3.11 (m, 12H), 2.12 (s, 18H), 1.82 (m, 24H), 1.52 (q, ^3J = 7.1 Hz, 24H), 1.04 (t, ^3J = 7.1 Hz, 36H). Elem anal. calcd for $C_{141}H_{228}EuN_9O_{30} \cdot 4CH_2Cl_2$: C, 57.65; H, 7.87; N, 4.17. Found: C, 57.35; H, 7.87; N, 4.17.

$[Bu_4N]_3[EuL^5_3]$. Orange oil, yield: 64%. NMR (200.13 MHz, CD_3OD): 6.78 (d, ^3J = 8.3 Hz, 6H), 6.49 (d, ^3J = 8.3 Hz, 6H), 4.24 (b, 6H), 3.38 (m, 114H), 1.75 (m, 24H), 1.47 (m, 24H), 1.03 (t, ^3J = 7.1 Hz, 36H). Elem anal. calcd for $C_{135}H_{216}N_9O_{30}Eu \cdot 4CH_2Cl_2$: C, 56.85; H, 7.69; N, 4.29. Found: C, 56.58; H, 7.76; N, 4.23.

$[Bu_4N]_3[EuL^6_3]$. Yield: 67%. NMR (200.13 MHz, CD_3OD): 7.85 (d, ^3J = 8.1 Hz, 6H), 7.64 (d, ^3J = 15.2 Hz, 3H), 7.50 (d, ^3J = 8.6 Hz, 6H), 7.32 (d, ^3J = 15.2 Hz, 3H), 7.18 (d, ^3J = 8.1 Hz, 6H), 6.75 (d, ^3J = 8.6 Hz, 6H), 4.53 (bs, 6H), 3.57 (m, 96H), 3.36 (m, 42H), 1.69 (m, 24H), 1.43 (m, 24H), 1.02 (t, ^{3}J= 7.1 Hz, 36H). Elem anal. calcd for $C_{174}H_{258}N_9O_{39}Eu \cdot 6CH_2Cl_2$: C, 59.90; H, 7.74; N, 3.49. Found: C, 59.45; H, 7.62; N, 3.37.

$[NBu_4]_3[Eu(L^7)_3]$. Orange oil, yield: 61%. ^{1}H NMR (200.13 MHz, CD_3OD): δ 6.23 (m, 12H), 4.12 (bs, 6H), 3.68 (m, 24H), 3.35 (m, 72H), 3.16 (s, 18H), 1.95 (m, 24H), 1.62 (m, 24H), 1.06 (t, ^3J = 7.0 Hz, 36H). ^{13}C NMR (50.332 MHz, CD_3OD): δ 164.4, 161.6, 149.3, 137.3 128.1, 118.5, 110.8, 71.4, 70.1, 69.9, 68.2, 58.6, 50.2, 23.8, 19.6, 12.8. Elem anal. calcd for $C_{129}H_{216}N_9O_{30}Eu \cdot 3CH_2Cl_2$: C, 57.03; H, 8.05; N, 4.53. Found: C, 56.59; H, 8.27; N, 4.26.

$[Bu_4N]_3[EuL^8_3]$. White oil, yield: 85%. NMR (200.13 MHz, $CDCl_3$): 7.46 (m, 9H), 7.05 (m, 9H), 5.15 (bs, 6H), 4.65 (m, 24H), 4.16 (m, 6H), 3.85 (m, 6H), 3.64 (m, 18H), 3.51 (m, 6H), 3.32 (s, 9H), 2.37 (m, 24H), 1.76 (m, 24H), 1.02 (m, 36H). Elem anal. calcd for $C_{126}H_{177}N_6O_{24}Eu \cdot 2CH_2Cl_2$: C, 61.95; H, 7.35; N, 3.39. Found: C, 61.89; H, 7.95; N, 3.39.

$[Bu_4N]_3[EuL^9_3]$. White oil, yield: 55% NMR (200.13 MHz, $CDCl_3$): 7.35 (d, ^3J = 8.9 Hz, 6H), 7.27 (d, 7.30 (m, 6H), 6.96 (d, ^3J = 8.3 Hz, 6H), 6.82 (d, ^3J = 8.9 Hz, 6H), 5.76 (b, 24H), 5.04 (s, 6H), H), 4.10 (m, 6H), 3.81 (t, ^3J = 5.0 Hz, 6H), 3.60 (m, 18H), 3.53 (m, 6H), 3.30 (s, 9H), 2.98 (b, 24H), 2.08 (b, 24H), 1.15 (t, ^3J = 6.7 Hz, 36H). Elem anal. calcd for $C_{138}H_{183}N_6O_{24}Eu \cdot 2CH_2Cl_2$: C, 63.89; H, 7.16; N, 3.19. Found: C, 64.05; H, 7.72; N, 3.17.

Acknowledgment. The authors are grateful to the French Agence Nationale de la Recherche (ANR LnOnL NT05-3_42676) for financial support. The authors also would like J. Bernard for technical assistance and Dr. M. Allali for help.

Supporting Information Available: Comparison of TPA spectra of $Na_3Eu\mathbf{L^{2G}}_3$ in water and DCM solution, photophysical and two-photon data for Eu complexes, and detailed synthesis procedures of the intermediate compounds. This material is available free of charge via the Internet at http://pubs.acs.org.

IC8012975